JOURNAL OF AGRICULTURAL AND FOOD CHEMISTRY

ARTICLE

pubs.acs.org/JAFC

Resveratrol Metabolites Do Not Elicit Early Pro-apoptotic Mechanisms in Neuroblastoma Cells

Jason D. Kenealey,[†] Lalita Subramanian,[§] Paul R. Van Ginkel,[§] Soesiawati Darjatmoko,[§] Mary J. Lindstrom,[#] Veronika Somoza,[⊥] Sunil K. Ghosh,[⊗] Zhenlei Song,[⊗] Richard P. Hsung,[⊗] Glen S. Kwon,[⊗] Kevin W. Eliceiri,[△] Daniel M. Albert,[§] and Arthur S. Polans*[,†,§]

[†]Department of Biomolecular Chemistry, Room 587, Medical Science Center, University of Wisconsin, 1300 University Avenue, Madison, Wisconsin 53705, United States

[§]Ophthalmology and Visual Sciences, University of Wisconsin, Suite 200, 2828 Marshall Court, Madison, Wisconsin 53705, United States

[#]Biostatistics and Medical Informatics, K6/446 Clinical Sciences Center, University of Wisconsin, 600 Highland Avenue, Madison, Wisconsin 53792, United States

[⊥]School of Medicine and Public Health, Institute of Nutritional and Physiological Chemistry, Althanstrasse 14 (UZA II), University of Vienna, Vienna, Austria

[⊗]Pharmaceutical Sciences Division, School of Pharmacy, University of Wisconsin, 777 Highland Avenue, Madison, Wisconsin 53705, United States

[△]Laboratory for Optical and Computational Instrumentation, College of Engineering, University of Wisconsin, 1415 Engineering Drive, Madison, Wisconsin 53706, United States

ABSTRACT: Resveratrol, a nontoxic polyphenol, has been shown to inhibit tumor growth in a xenograft mouse model of neuroblasoma. However, resveratrol is rapidly metabolized, mainly to its glucuronidated and sulfated derivatives. This study demonstrates that resveratrol alone, and not the glucuronidated or sulfated metabolites, is taken up into tumor cells, induces a rise in $[Ca^{2+}]_i$, and ultimately leads to a decrease in tumor cell viability. A new water-soluble resveratrol formulation was delivered directly at the site of the tumor in a neuroblastoma mouse model. The amount of unmodified resveratrol associated with the tumor increased more than 1000-fold. The increase of unmodified resveratrol associated with the tumor resulted in tumor regression. The number of residual tumor cells that remained viable also decreased as the ratio of the metabolites relative to unmodified resveratrol declined.

KEYWORDS: resveratrol, neuroblastoma, calcium signaling, bioavailability

INTRODUCTION

Over the past several decades researchers have focused on finding drugs that specifically affect cancer cells without harming normal cells. Often this research has focused on naturally occurring compounds. Jang et al.[1] found that resveratrol (Res), a natural product found in grapes, peanuts, and Japanese knotweed, could prevent cancer in a mouse model of melanoma. Following this initial study the anticancer effect of Res has been studied in a variety of cancers. In this study we focus on neuroblastoma, a childhood cancer that most often arises in the sympathetic nerves of the adrenal gland and accounts for 15% of the childhood deaths from cancer.[2,3] Despite aggressive combination therapeutic approaches, more than 60% of the children with high-risk neuroblastoma do not survive due to metastasis, high recurrence, and chemoresistance. Between 20 and 50% of high-risk cases do not respond adequately to induction high-dose chemotherapy and are progressive or refractory. Relapse after completion of frontline therapy is also common. Furthermore, the quality of life of these children is threatened by therapy-induced toxicity.[4] Thus, these children would benefit from a nontoxic compound, such as resveratrol, to alleviate the devastating side effects of standard therapeutics.

In vitro mechanistic studies have indicated that Res can activate pathways implicated in apoptosis.[5] However, in mouse xenograft models, in which Res has been shown to inhibit tumor growth when delivered orally, there is little evidence of apoptosis. One possible explanation for the absence of apoptosis in these mouse models is the low bioavailability of Res. The inhibition of tumor growth achieved at lower levels of resveratrol could be explained by other mechanisms of action, including antiproliferative and antiangiogenic activities.[6]

In vivo studies in animals and humans indicate that resveratrol is poorly absorbed from the gastrointestinal tract and undergoes extensive first-pass metabolism, mainly glucuronidation and sulfation, in the gut and liver, leading to trace amounts of the compound in the serum. The resveratrol metabolites are then dependent on ABC transporters for uptake.[7−10] Our previous studies in neuroblastoma indicate that despite low bioavailability, resveratrol is effective at inhibiting tumor growth when delivered orally.[5] Indeed, when the serum levels of Res were measured in

Received: December 21, 2010
Revised: March 8, 2011
Accepted: March 14, 2011
Published: March 14, 2011

dx.doi.org/10.1021/jf104901g | *J. Agric. Food Chem.* 2011, 59, 4979–4986

such rodent studies, there was <1 μM Res and 20-fold higher levels of the Res metabolites within 0.5 h of drug delivery.

The anticancer properties of Res could result either from activation of pathways through extracellular receptors or uptake into cells and activation of intracellular regulators. Currently, the only evidence for entry of Res into cells comes from cell types that have specialized uptake mechanisms.[11] Determining the subcellular localization of Res would help elucidate potential binding partners and mechanisms whereby Res induces tumor cell death. We therefore want to investigate how Res and its metabolites might differ in cellular uptake, pathway activation, and ultimately tumor cell death. An early pathway activated by Res, in tumor cells, is calcium signaling by increasing cytoplasmic calcium.[12] Calcium signaling plays a vital role in cell proliferation, angiogenesis, and cell death.[13] The versatility of calcium signaling is due to the cell's ability to control the localization and concentration of the signal and the array of responsive calcium binding proteins in the cell. A sustained increase in $[Ca^{2+}]_i$ in tumor cells is thereby associated with the activation of pathways leading to inhibition of tumor cell proliferation as well as cell death.[14] Previous studies [15,16] have shown that chelating $[Ca^{2+}]_i$ with BAPTA-AM inhibits the Res-induced tumor cell death.

In this study we demonstrate that Res enters neuroblastoma cells, induces a calcium signal, and ultimately decreases tumor cell viability. Both Res uptake and ER calcium release occur within minutes of drug exposure. Meanwhile, we present evidence using purified derivatives that Res's sulfated and glucuronidated metabolites are not taken up by neuroblastoma cells and, therefore, are incapable of activating calcium signals. Consequently, the Res metabolites have no impact on the viability of these cells. Therefore, metabolism diminishes Res's anticancer effects. As proof of principle, we demonstrate a method of Res delivery that reduces its rapid metabolism to achieve apoptosis and tumor regression in a neuroblastoma mouse model.

MATERIALS AND METHODS

Materials. Purified resveratrol was purchased from Cayman Chemical (Ann Arbor, MI). Fura-2 was purchased from Molecular Probes. Pluronic P104 was kindly donated by BASF (BASF, Mount Olive, NJ). All other chemicals were of reagent grade. Athymic nu/nu mice were purchased from Harlan Sprague−Dawley Inc. (Indianapolis, IN). Animals were housed in a pathogen-free isolation facility. All animal care and treatment protocols were in compliance with guidelines and approved by the University of Wisconsin—Madison Animal Care and Use Committee.

Cell Culture. SK-N-AS and NGP neuroblastoma cell lines were grown as adherent cells at 37 °C, 5% CO_2 in RPMI 1640 supplemented with 10% (v/v) fetal bovine serum (Atlanta Biologicals, Lawrenceville, GA), 10 mmol/L HEPES, and 1% penicillin−streptomycin−amphotericin B (Sigma, St. Louis, MO).

Res Formulation Containing P104 (R-P104). Two hundred microliters of ethanol (2%) was added to 20 mg of Res, then dissolved in 10 mL of a 10% P104 aqueous solution, and filtered through a 0.2 μm syringe filter to obtain a clear pale yellow solution. The concentration of Res in the solution was quantified by HPLC prior to use (see below).

In Vitro Cell Viability. Cells were grown in 96-well microtiter plates for 2 days. Drug treatments were started, and corresponding treatment media were replenished after 2 days. Four days later Cell Titer Blue reagent was added according to the manufacturer's instructions (Promega, Madison, WI). Fluorescence was measured at excitation/emission wavelengths of 560/590 nm, using a fluorescence plate reader (Molecular Devices, Sunnyvale, CA).

Calcium Imaging. Cells were imaged following a standard protocol.[12] Briefly, neuroblastoma cells were loaded with fura-2-AM for 30 min at 37 °C followed by a 30 min incubation at room temperature. Cells were subsequently imaged on the BD Pathway microscope. The fura-2 loaded cells were alternately excited at 340 and 380 nm and emission was monitored at 510 nm. Drugs were added following 40 s of baseline collection, and the average fluorescence output was converted to average calcium concentration via the Grynkiewicz equation.[17]

Two-Photon Microscopy. A custom multiphoton workstation at the University of Wisconsin Laboratory for Optical and Computational Instrumentation (LOCI, www.loci.wisc.edu) was utilized. All samples were imaged with the same power using a TE300 inverted microscope (Nikon, Tokyo, Japan) equipped with a CFI Plan Fluor 20x (N.A. = 1.2; Nikon) objective lens by using a mode-locked Ti:sapphire laser (Spectra Physics Mai Tai, Mountain View, CA). An excitation wavelength of 765 nm was used to detect the fluorescence signal using a H7422P GaAsP photon counting PMT (Hamamatsu, Hamamatsu City, Japan). Cells were incubated at 37 °C using a stage incubator. Images of 1024 × 1024 pixels were acquired using WiscScan (http://www.loci.wisc.edu/wiscscan/) under identical conditions and laser power.

Animal Studies. Twenty-one 5−6-week-old female athymic nu/nu mice were each given a dorsal subcutaneous injection of SK-N-AS neuroblastoma cells (3×10^6) suspended in 500 μL of 1:1 culture medium and basement membrane matrix suspension (BD Matrigel; Fisher Scientific, Pittsburgh, PA). Tumors were allowed to grow for 4 days before the randomization of the animals into four groups of five animals each. Tumors were allowed to grow to approximately 200 mm^3 before starting administration of five injections of 200 μL of R-P104 (approximately 5 mg of Res per injection) or vehicle over a period of 2 weeks either in the tissue adjacent to the tumor (peri-tumor) or into the tumor (intratumor). Tumor volume was measured twice a week in three dimensions with calipers, and the volume was approximated by multiplying the three measurements. On the day after the last dose, the animals were euthanized and photographed, and their tumors were harvested, measured in three dimensions using calipers, fixed in 10% neutral buffered formalin, and processed for histology. Five-micrometer sections were cut in a masked fashion to obtain sections that encompassed the full circumference of the tumor that were then stained with hematoxylin−eosin (H&E). These were examined microscopically, and the histopathologic features were recorded as previously described.[18−20] Histopathology and tumor section evaluations were carried out independently by two trained observers (D.M.A. and P.v.G.). The percentage of the tumor that was necrotic (percent necrotic area) in R-P104- and vehicle-treated tumors was determined in H&E-stained tumor sections. The outline of the tumor in each section was traced from a microscopically digitized image, and the areas of viable- and nonviable-appearing tumor were measured using ImageJ software (Wayne Rasband, NIH, rsbweb freeware).

Statistical Analysis. All data were analyzed using one-way ANOVA. If this initial analysis found a significant difference among the groups, then *t* tests were used to test for pairwise differences between groups. All responses were transformed to the log scale to obtain data that satisfy the assumptions required for ANOVA. Means and standard errors (SE) were calculated by transforming back from the log scale. Differences were considered to be significant at $P < 0.05$.

Bioavailability: Serum Measurements. SKNAS cells were implanted in the flanks of nude mice as described in the animal studies, and tumors were allowed to grow to >200 mm^3. A single dose of 5 mg of R-P104 was administered to three mice each by oral gavage or by peritumor or intratumor injection. Blood was extracted from the axillary vessels at 30 min after drug administration before the mice were euthanized. Serum and tumors were collected, and HPLC measurements were carried out using standard procedures.[5] Briefly, samples from each

Scheme A. Chemical Syntheses of C3-Unprotected Res (1), C4-Unprotected Res (2), and Trifluoromethyl Amidate (7)

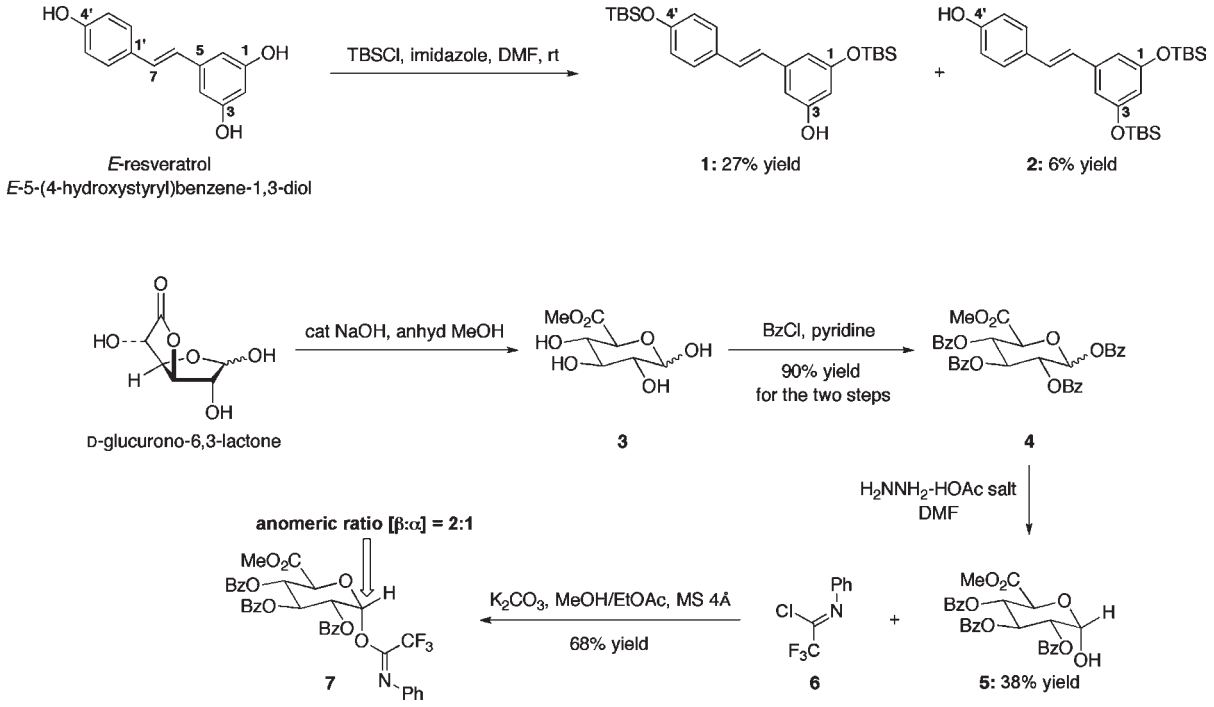

mouse were divided into two equal parts. One part was used to measure the concentration of unmetabolized Res. The other part was treated with 10000 U/mL β-glucuronidase (type IX-A, *Escherichia coli*, Sigma) and 50 μL of sulfatase (type VI, *Aerobacter aerogenes*, Sigma) to determine the total concentration of Res (metabolized and unmetabolized). All samples were then incubated at 37 °C for 5 h and extracted with 2 × 0.5 mL of ethyl acetate. Upper phases were mixed, and the solvent was evaporated. The residual pellets were dissolved in 0.05 mL of HPLC solvent B. These samples were then analyzed by the HPLC method to quantify Res concentrations in the serum samples. As an additional control, Res-spiked serum was analyzed and found to be extracted with 90% efficiency.

HPLC Method. Samples were analyzed by reverse-phase HPLC using a Gemini C6-phenyl column (4.5 × 250 mm) with 5 μm particle size (Phenomenex, Torrance, CA). The mobile phase consisted of a 40:60 mixture of solvent A (0.1% trifluoroacetic acid in water) and solvent B (90% acetonitrile/10% water/0.09% trifluoroacetic acid) pumped at 1 mL/min. The eluent was monitored at 305 nm. Calibration curves were obtained using resveratrol standard solutions (0−2000 pmol) and found to be linear with a correlation coefficient of >0.99.

Synthesis of Resveratrol Metabolites. Preparations of 3-O and 4′-O-glucuronidated Res derivatives (3-OGR and 4′-OGR) could be readily accomplished utilizing the synthetic sequences shown in Schemes A and B. Crude products were further purified using a preparative Gemini C6 phenyl HPLC column (Phenomenex, 5 μm, 105 Å, 250 × 10 mm). A gradient program was set starting with a 50% mix of solvents A and B linearly increasing to 60% B at 3 min, 65% B at 10 min, and 100% B at 15 min, followed by 50% B at 17 min. At a flow rate of 3 mL/min, the main fraction for the 4′-OGR eluted at 4 min, the 3-OGR at 5 min, and Res at 7 min. Purification yielded desired products of ∼90% purity. Res 3-*O*-sulfate (monosulf-Res) and the combination of Res 3-*O*-4′-*O*-disulfate and 3-*O*-5-*O*-disulfate (disulf-Res) were synthesized according to published procedures.[21]

RESULTS AND DISCUSSION

Resveratrol Metabolites Effect on Neuroblastoma Cell Viability in Vitro. Within minutes after ingestion, Res is predominantly recovered in the serum as sulfated and/or glucuronidated metabolites. The role of these metabolites in the anticancer effect of Res is not well understood. Therefore, we initially treated neuroblastoma cells with 100 μM Res or 100 and 200 μM 3- and 4′-OGR as well as mono- and disulf-Res for 4 days and then normalized their responses to DMSO controls (Figure 1). Unmodified Res reduces the number of viable cells by ∼85%. However, the metabolites, even at considerably higher concentrations, have no effect on viability, indicating that the metabolites do not induce tumor cell death or prevent their proliferation in vitro. These findings are consistent with another report that mono- and disulf-Res have considerably lower potency compared to resveratrol in determining the viability of breast cancer cells.[22]

Resveratrol Uptake. Direct binding targets contributing to the anticancer properties of Res are yet to be definitively identified. One obstacle to finding sentinel binding targets for Res is the uncertainty of whether or not Res enters tumor cells. Res is a weak fluorophore with an excitation maximum at 320 nm and emission at 390 nm. In the findings reported here, Res fluorescence was utilized in multiphoton microscopy[23] to observe the cellular localization of Res in neuroblastoma cells. Multiphoton microscopy has the ability to detect weak signals at low wavelengths (broad tunability down to 765 nm for Res and 780 nm for optimized autofluorescence) without significant photobleaching or cytotoxicity. Figure 2A shows representative optically sectioned slices of cells treated with Res. These images indicate that Res enters and then permeates throughout the cell. Low background autofluorescence attributed to NADH is visible at 765 nm (Figure 2B,i), but within 90 s of the addition of Res, the

Scheme B. Chemical Syntheses of 3- and 4′-Glucuronidated Res Derivatives 3-OGR and 4′-OGR

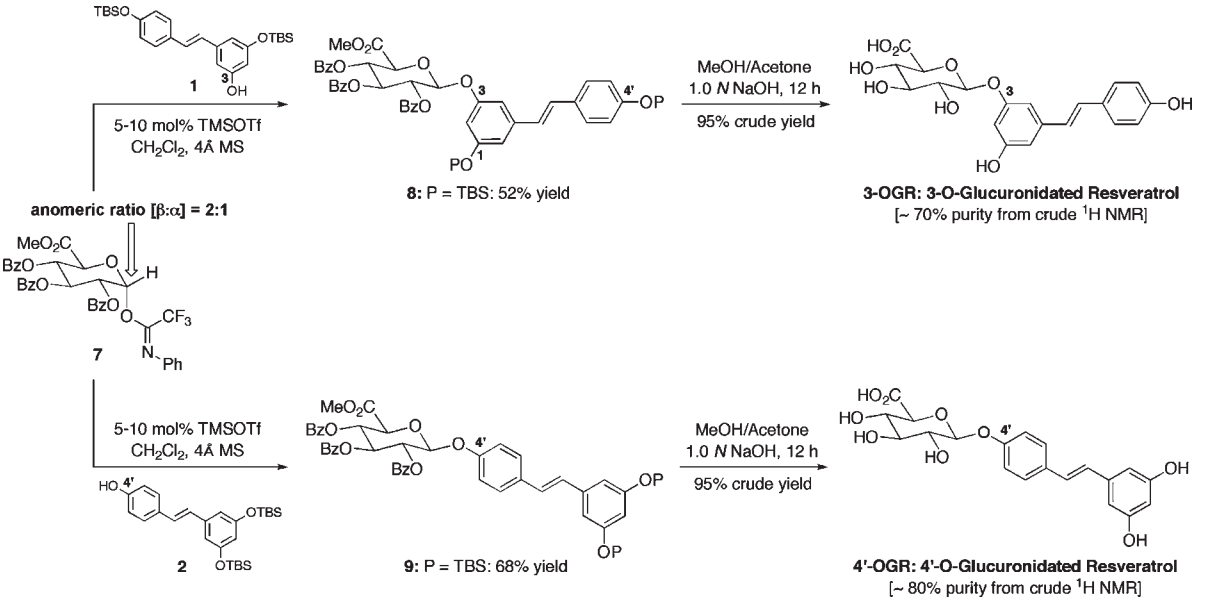

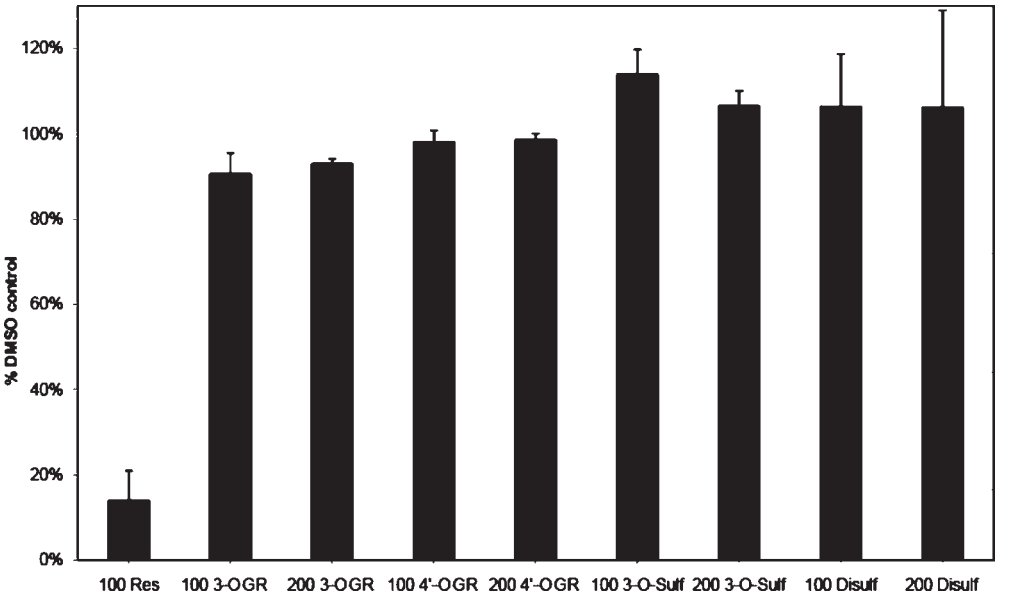

Figure 1. Viability of neuroblastoma cells treated with Res or the Res metabolites: 3-O- and 4′-O-glucoronidated Res and 3-O- and disulfated Res. Neuroblastoma cells were treated with 100 μM Res or 100 or 200 μM Res metabolites for 4 days before viability was measured using Cell Titer Blue. Each experiment was done in triplicate and repeated twice.

cells become brightly fluorescent (Figure 2B,ii). This suggests that the rate of accumulation of Res is quite rapid at 37 °C as is the rate of depletion when Res is removed from the extracellular milieu (Figure 2B,iii). The process is shown to be reversible when the cells again fluoresce on readdition of Res (Figure 2B,iv). Given the current configuration of the multiphoton microscope, 90 s following the addition of Res is the earliest time point that can be taken. At this time Res is observed throughout the cytosol, indicating that Res is taken up within this period of time and likely much more rapdily. Res washes out within a similar time frame, indicating that cellular uptake of Res is reversible.

The glucuronidated and sulfated metabolites of Res have fluorescence spectra similar to the spectrum of Res with comparable fluorescence intensity. However, when the metabolites were added to the tumor cells (Figure 2C), there was no observable change in cellular fluorescence. This suggests that the uptake mechanism of the metabolites (if any) in tumor cells is quite different from that of Res.

These data indicate that resveratrol and not its metabolites enter neuroblastoma cells and that metabolites are unlikely to contribute to the subsequent intracellular events shown below. It may be possible that in other cell types resveratrol is converted

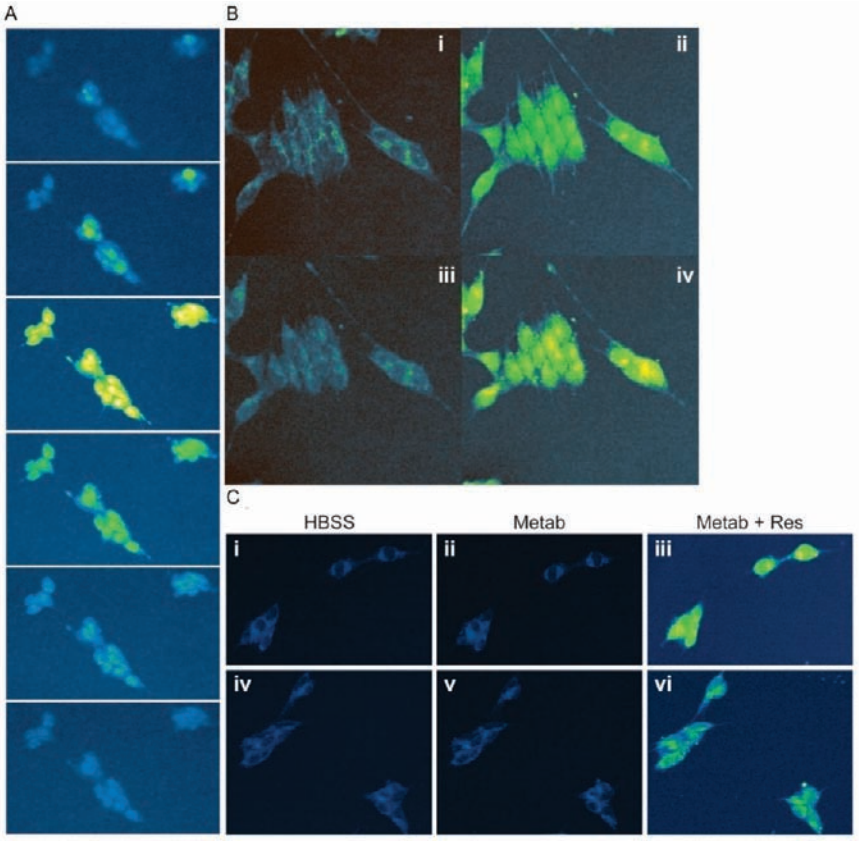

Figure 2. Res's cellular uptake determined by live-cell multiphoton microscopy excited at 765 nm at 37 °C. (A) Neuroblastoma cells were treated with Res and subsequently imaged in 2 μm step optical sections. Shown are representative sections through the cells (sections 1, 3, 10, 12, 14, and 16). (B, i) Cells in Hanks balanced salt solution (HBSS) were excited at 765 nm to show autofluorescence. (B, ii) The cells from panel B,i were similarly imaged 5 min following the addition of 100 μM RES. (B, iii) Cells were washed with HBSS to remove Res and imaged again after 5 min. (B, iv) Res was readded to the cells, which leads to an increase in cytoplasmic fluorescence. (C) Neuroblastoma cells were imaged at 765 nm in HBSS (i, iv), with Res metabolites (100 μM disulf-Res), (ii) with 100 μM gluc-Res, and (v) with 100 μM Res plus respective metabolites (iii and vi).

within cells to metabolites that may then activate anticancer events.[24] However, when SK-N-AS cells were incubated with resveratrol for 0.5−72 h, no metabolites could be detected in either the media or cell extracts (data not shown). Therefore, the studies presented here demonstrate that unmodified resveratrol is needed for transport into tumor cells and that the unmodified compound is likely responsible for the activation of subsequent intracellular events leading to tumor cell death.

Resveratrol-Induced Calcium Flux. Res has been shown to induce apoptosis in a variety of cancer cell lines. Although many potential targets have been evaluated, Res's mechanism of action remains unclear. A rise in $[Ca^{2+}]_i$ has been shown as an early event in apoptotic pathways. A previous study in breast cancer shows that Res induces a rise in $[Ca^{2+}]_i$ that activates the intrinsic mitochondrial apoptotic pathway leading to the activation of caspases and calpain and ultimately to tumor cell death.[12] To determine whether Res metabolites induce a calcium response in tumor cells, neuroblastoma cells were loaded with the ratiometric calcium indicator fura-2. Addition of Res (Figure 3) caused an increase in fluorescence, reflecting the rise in $[Ca^{2+}]_i$. The change in fura-2 fluorescence could be suppressed when the cells were coloaded with the calcium chelator BAPTA-AM, suggesting that resveratrol-induced changes to fura-2 fluorescence correlate with changes in intracellular calcium levels (data not shown). As seen in Figure 3, none of the Res metabolites evoked a fura-2 fluorescence change, indicating that the metabolites did not activate calcium release. Combined with the lack of observable cell death in the tumor cells as described earlier, it would appear that the metabolites are incapable of activating the intrinsic mitochondrial apoptotic pathway in vitro.

These in vitro studies comparing Res with its glucuronidated and sulfated metabolites suggest that metabolism results in decreased cellular uptake and a corresponding lack of activation of the pathways critical to the anticancer activity of Res. Therefore, improved efficacy of Res as an anticancer drug would depend on the availability of higher levels of free (unmetabolized) Res and lower levels of metabolites in the tumor environment.

Bioavailability of Res. Res is typically administered in an "oil-based" vehicle in oral efficacy studies in animal models of different types of cancer.[25] We have determined that even at doses of 50 mg/kg in such vehicles, the serum level of free Res is <1 μM (0.5 μM typically) and tumors are associated with 0.001 μmol/g Res at peak accumulation. The combined metabolites in the serum are 10−20-fold higher (25 μM) in concentration than free Res under these conditions. To achieve higher levels of Res relative to the metabolites, a water-soluble formulation of Res using a block copolymer was prepared. This formulation allowed us to compare the bioavailability of Res at higher doses (250 mg/kg) administered orally, injected next to the tumor (peritumor) or directly into the tumor (intratumor). The levels of Res in the

serum and tumor were determined after a single dose. Using the formulation, free Res levels in the serum increased to >10 μM for all three delivery routes (Table 1) with 10-fold lower metabolite concentrations in the peri- and intratumor injections (20 and 34 μM, respectively) than oral delivery (325 μM). Oral delivery also resulted in 87% of the Res associated with the tumor being composed of metabolites and only 0.007 μmol/g of free Res. As anticipated, direct injections resulted in much higher concentrations of Res associated with the tumor. Peritumor injections resulted in free Res amounts of 6 μmol/g and a lower percentage of metabolites (50%). Intratumor injections provided the best results, with 11 μmol/g of free Res associated with the tumor and only 15% of the Res in the metabolized forms.

As proof of principle that elevated levels of free Res rather than the metabolites are necessary to achieve a potent antitumor effect, peritumor and intratumor injections of 250 mg/kg Res in the water-soluble formulation were tested using a neuroblastoma xenograft mouse model.

In Vivo Efficacy. First, to test whether tumor inhibition can be achieved with injections of Res, we conducted the experiment using SK-N-AS cells in athymic mice. Tumors were allowed to grow to an approximate volume of 200 mm^3 before the start of a series of 5 peri- or intratumor injections, each of 200 μL of R-P104 (approximately 5.0 mg of Res per injection) or vehicle over 2 weeks. Mean tumor size in each group over the course of the study was plotted (Figure 4A) to compare the rate of growth of the tumors in the two groups. In the peritumor-injected mice, Res treatment showed tumor inhibition of about 88% compared to vehicle-treated controls (p = 0.003). The average tumor volumes of the treated group after five doses of R-P104 was 145.8 mm^3 (SE = 54.13 mm^3), whereas the tumors in the control group grew to an average volume of 1195.4 mm^3 (SE = 506 mm^3). Intratumor injections resulted in similar tumor volumes (treated = 177 mm^3, SE = 46 mm^3; control = 612 mm^3, SE = 46 mm^3; p value = 0.0036). Next, tumor sections were H&E-stained and viable areas (intact cells with large pleomorphic nuclei that stained predominantly with hematoxylin) were measured with ImageJ software. Analysis of the tumor sections from the peritumor-injected mice revealed that both drug- and vehicle-treated groups of mice contained areas of decomposing cells showing eosinophilic staining (Figure 4B). This appearance is typically associated with rapidly growing tumors that have outstripped their blood supply. However, in addition to the smaller tumor size in the treated group, on average only 35% of the tumor (21−49%) appeared viable compared to 68% (60−73%) in the vehicle-treated controls, indicating that there was increased cell death related to treatment. Microscopic evaluation showed areas of apoptotic cells with pyknotic nuclei in the drug-treated tumors.

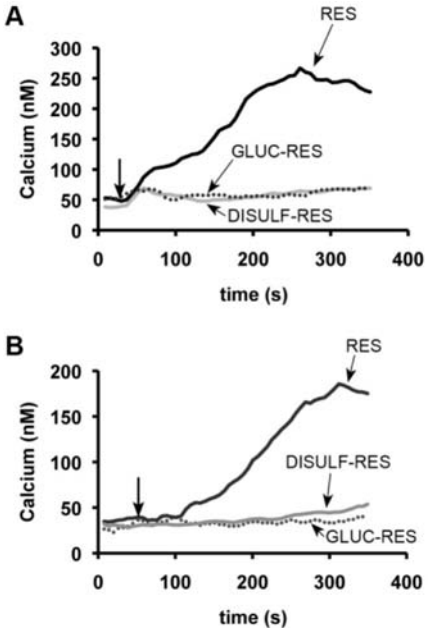

Figure 3. Res-induced calcium flux in neuroblastoma cells. Neuroblastoma cells, SK-N-AS (A) and NGP (B), were placed on 96-well plates and loaded with fura-2. Live-cell microscopy was used to detect the change in $[Ca^{2+}]_i$. A baseline $[Ca^{2+}]_i$ was established for 40 s followed by the addition of 100 μM Res (solid black), 100 μM gluc-Res (dotted), or 100 μM disulfated Res (light gray) as indicated by the arrow. (The same results were obtained with 3-O-sulfated Res.)

Tumor sections from the intratumor-injected group suggested improvement over peritumor injections with an even smaller percentage of viable areas in the treated tumors. On average only about 8% (0−25%) of the tumor was viable in R-P104-treated tumors compared to 55% (30−69%) in the vehicle-treated tumors when viable areas were quantified using ImageJ software on the H&E-stained tumor sections. Microscopic evaluation showed extensive areas of necrosis with ghost cells and liquified cell material interspersed with apoptotic cells with pyknotic nuclei in the drug-treated tumors that are absent in the vehicle-treated tumors. Therefore, even though tumor volume measurements showed inhibition of tumor growth in both the peritumor and intratumor models, the histopathology evaluation of the residual tumors suggested the potential for tumor regression and increased potency with intratumor injections (Figure 4C).

In contrast, daily oral administration of Res in mice has been shown to result in submicromolar serum levels of Res and elevated levels of metabolites.[26] These low concentrations of resveratrol are still able to inhibit tumor growth, most likely by inhibiting cell proliferation or tumor angiogenesis. However, these low levels of resveratrol are insufficient to activate tumor cell apoptosis, and thus tumor regression is not observed. By solubilizing Res using a block copolymer to enable administration of higher doses (250 mg/kg), we were able to establish that

Table 1. Bioavailability of 5 mg of Res-P104 after 30 min

	oral		peri		intra	
	resveratrol	metabolites	resveratrol	metabolites	resveratrol	metabolites
serum (μM)	11	325	14	20	13	34
%	3	97	41	59	28	72
tumor (μmol/g)	0.007	0.046	5.3	6.4	10.9	1.9
%	13	87	45	55	85	15

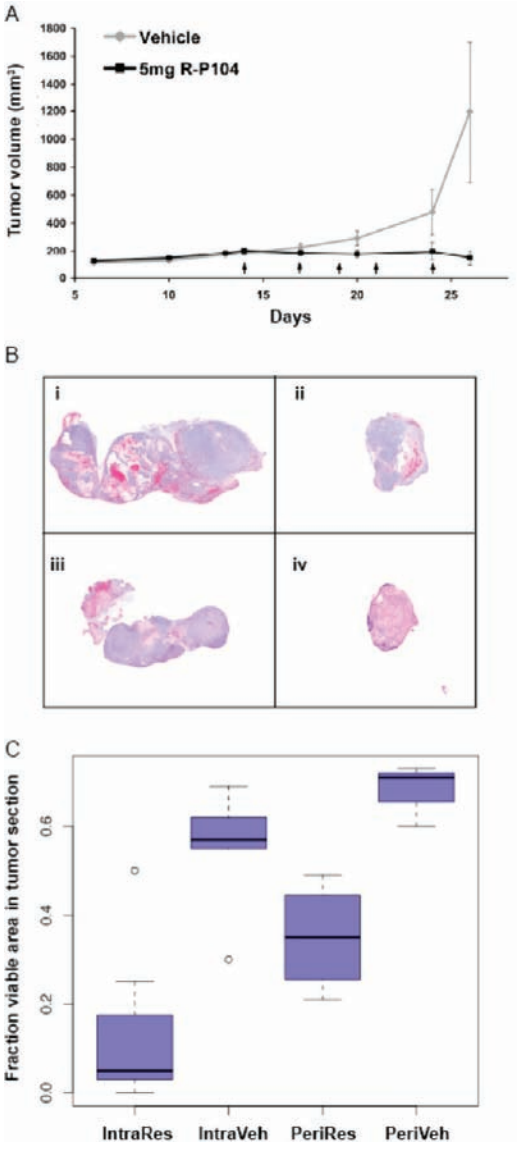

Figure 4. Res inhibits tumor growth in a xenograft mouse model and induces tumor regression when the concentration of unmetabolized Res in the tumor is increased. (A) Tumor growth kinetics during R-P104 treatment course of a SK-N-AS xenograft model by peritumor injections. Plotted is the change in average tumor volume in R-P104-treated and vehicle-treated groups of mice. Each arrow indicates a single 200 μL dose. (B) Neuroblastoma tumor histology. H&E-stained paraffin sections of tumors were removed from mice after five (i) vehicle-treated peritumor, (ii) R-P104-treated peritumor, (iii) vehicle-treated intratumor, or (iv) R-P104-treated intratumor injections. (Hematoxylin stains blue, and eosin stains red.) (C) Plot of average percent viable area in each tumor section from treated and untreated animals. Three sections from each tumor and five tumors per group were used to calculate the averages.

direct injection of Res into the tumor resulted in the highest levels of free Res in the serum and tumor; regression of the tumor was then observed. In a new study resveratrol was delivered by peritumor injection in a syngeneic mouse model of neuroblastoma, to cause tumor regression.[27] Subsequent immunotherapy then proved to be more effective, resulting in a significant improvement in life expectancy. The achievement of tumor regression observed in both of these studies is potentially important, because neuroblastoma arises primarily in the abdominal region as a consequence of sympathetic innervations of the adrenal gland and, therefore, injections are quite feasible to reduce tumor burden as either a primary or neoadjuvant treatment. In addition, by achieving both higher levels of free Res and significant improvements in tumor cell death, these findings support our in vitro data that free Res is more directly responsible for antitumor activity.

AUTHOR INFORMATION

Corresponding Author

*Postal address: M. D. Matthews Retina Research Foundation Professor, Department of Ophthalmology and Visual Sciences, Room K6/466 Clinical Sciences Center, University of Wisconsin, 600 Highland Avenue, Madison, WI 53792. Phone: (608) 265-4423. Fax: (608) 265-6021. E-mail: aspolans@wisc.edu.

Funding Sources

This work was supported by grants from the National Institutes of Health, R01CA103653 (A.S.P.), the Retina Research Foundation (A.S.P. is the M. D. Matthews Retina Research Foundation Professor), the Mandelbaum Cancer Therapeutics Initiative (A.S.P. and D.M.A.), the American Institute for Cancer Research (P.v.G.), and the UW Carbone Comprehensive Cancer Center (R.P.H.).

ACKNOWLEDGMENT

We thank Chue Vang for excellent technical assistance.

ABBREVIATIONS USED

Res, resveratrol; $[Ca^{2+}]_i$, intracellular calcium concentration; R-P104 , resveratrol P104 formulation; 3-OGR, 3-O-glucuronidated resveratrol; 4′-OGR, 4′-O-glucuronidated resveratrol.

REFERENCES

(1) Jang, M.; Cai, L.; Udeani, G. O.; Slowing, K. V.; Thomas, C. F.; Beecher, C. W.; Fong, H. H.; Farnsworth, N. R.; Kinghorn, A. D.; Mehta, R. G.; Moon, R. C.; Pezzuto, J. M. Cancer chemopreventive activity of resveratrol, a natural product derived from grapes. *Science* **1997**, *275* (5297), 218−220.

(2) Goldsby, R. E.; Matthay, K. K. Neuroblastoma: evolving therapies for a disease with many faces. *Paediatr. Drugs* **2004**, *6*, 107–122.

(3) Park, J. R.; Eggert, A.; Caron, H. Neuroblastoma: biology, prognosis, and treatment. *Pediatr. Clin. North Am.* **2008**, *55*, 97–120.

(4) Laverdiere, C.; Liu, Q.; Yasui, Y.; Nathan, P. C.; Gurney, J. G.; Stovall, M.; Diller, L. R.; Cheung, N. K.; Wolden, S.; Robison, L. L.; Sklar, C. A. Long-term outcomes in survivors of neuroblastoma: a report from the Childhood Cancer Survivor Study. *J. Natl. Cancer Inst.* **2009**, *101*, 1131–1140.

(5) van Ginkel, P. R.; Sareen, D.; Subramanian, L.; Walker, Q.; Darjatmoko, S. R.; Lindstrom, M. J.; Kulkarni, A.; Albert, D. M.; Polans, A. S. Resveratrol inhibits tumor growth of human neuroblastoma and mediates apoptosis by directly targeting mitochondria. *Clin. Cancer Res.* **2007**, *13*, 5162–5169.

(6) Gupta, S. C.; Kannappan, R.; Reuter, S.; Kim, J. H.; Aggarwal, B. B. Chemosensitization of tumors by resveratrol. *Ann. N.Y. Acad. Sci.* **2011**, *1215*, 150–160.

(7) Wenzel, E.; Soldo, T.; Erbersdobler, H.; Somoza, V. Bioactivity and metabolism of *trans*-resveratrol orally administered to Wistar rats. *Mol. Nutr. Food Res.* **2005**, *49*, 482–494.

(8) Marier, J. F.; Vachon, P.; Gritsas, A.; Zhang, J.; Moreau, J. P.; Ducharme, M. P. Metabolism and disposition of resveratrol in rats: extent of absorption, glucuronidation, and enterohepatic recirculation

evidenced by a linked-rat model. *J. Pharmacol. Exp. Ther.* **2002**, *302*, 369–373.

(9) Miksits, M.; Maier-Salamon, A.; Aust, S.; Thalhammer, T.; Reznicek, G.; Kunert, O.; Haslinger, E.; Szekeres, T.; Jaeger, W. Sulfation of resveratrol in human liver: evidence of a major role for the sulfotransferases SULT1A1 and SULT1E1. *Xenobiotica* **2005**, *35*, 1101–1119.

(10) van de Wetering, K.; Burkon, A.; Feddema, W.; Bot, A.; de Jonge, H.; Somoza, V.; Borst, P. Intestinal breast cancer resistance protein (BCRP)/Bcrp1 and multidrug resistance protein 3 (MRP3)/Mrp3 are involved in the pharmacokinetics of resveratrol. *Mol. Pharmacol.* **2009**, *75*, 876–885.

(11) Maier-Salamon, A.; Hagenauer, B.; Wirth, M.; Gabor, F.; Szekeres, T.; Jager, W. Increased transport of resveratrol across monolayers of the human intestinal Caco-2 cells is mediated by inhibition and saturation of metabolites. *Pharm. Res.* **2006**, *23*, 2107–2115.

(12) Sareen, D.; Darjatmoko, S. R.; Albert, D. M.; Polans, A. S. Mitochondria, calcium, and calpain are key mediators of resveratrol-induced apoptosis in breast cancer. *Mol. Pharmacol.* **2007**, *72*, 1466–1475.

(13) Berridge, M. J.; Lipp, P.; Bootman, M. D. The versatility and universality of calcium signalling. *Nat. Rev. Mol. Cell Biol.* **2000**, *1*, 11–21.

(14) Pinton, P.; Giorgi, C.; Siviero, R.; Zecchini, E.; Rizzuto, R. Calcium and apoptosis: ER-mitochondria Ca^{2+} transfer in the control of apoptosis. *Oncogene* **2008**, *27*, 6407–6418.

(15) Ma, X.; Tian, X.; Huang, X.; Yan, F.; Qiao, D. Resveratrol-induced mitochondrial dysfunction and apoptosis are associated with Ca(2+) and mCICR-mediated MPT activation in HepG2 cells. *Mol. Cell. Biochem.* **2007**, *302*, 99–109.

(16) Guha, P.; Dey, A.; Dhyani, M. V.; Sen, R.; Chatterjee, M.; Chattopadhyay, S.; Bandyopadhyay, S. K. Calpain and caspase orchestrated death signal to accomplish apoptosis induced by resveratrol and its novel analog hydroxystilbene-1 [correction of hydroxstilbene-1] in cancer cells. *J. Pharmacol. Exp. Ther.* **2010**, *334*, 381–394.

(17) Grynkiewicz, G.; Poenie, M.; Tsien, R. Y. A new generation of Ca^{2+} indicators with greatly improved fluorescence properties. *J. Biol. Chem.* **1985**, *260*, 3440–3450.

(18) Albert, D. M.; Kumar, A.; Strugnell, S. A.; Darjatmoko, S. R.; Lokken, J. M.; Lindstrom, M. J.; Patel, S. Effectiveness of vitamin D analogues in treating large tumors and during prolonged use in murine retinoblastoma models. *Arch. Ophthalmol.* **2004**, *122*, 1357–1362.

(19) Grostern, R. J.; Bryar, P. J.; Zimbric, M. L.; Darjatmoko, S. R.; Lissauer, B. J.; Lindstrom, M. J.; Lokken, J. M.; Strugnell, S. A.; Albert, D. M. Toxicity and dose-response studies of 1α-hydroxyvitamin D2 in a retinoblastoma xenograft model. *Arch. Ophthalmol.* **2002**, *120*, 607–612.

(20) Sabet, S. J.; Darjatmoko, S. R.; Lindstrom, M. J.; Albert, D. M. Antineoplastic effect and toxicity of 1,25-dihydroxy-16-ene-23-yne-vitamin D3 in athymic mice with Y-79 human retinoblastoma tumors. *Arch. Ophthalmol.* **1999**, *117*, 365–370.

(21) Wenzel, E.; Soldo, T.; Erbersdobler, H.; Somoza, V. Bioactivity and metabolism of trans-resveratrol orally administered to Wistar rats. *Mol. Nutr. Food Res.* **2005**, *49*, 482–494.

(22) Miksits, M.; Wlcek, K.; Svoboda, M.; Kunert, O.; Haslinger, E.; Thalhammer, T.; Szekeres, T.; Jager, W. Antitumor activity of resveratrol and its sulfated metabolites against human breast cancer cells. *Planta Med.* **2009**, *75*, 1227–1230.

(23) Zipfel, W. R.; Williams, R. M.; Webb, W. W. Nonlinear magic: multiphoton microscopy in the biosciences. *Nat. Biotechnol.* **2003**, *21*, 1369–1377.

(24) Murias, M.; Miksits, M.; Aust, S.; Spatzenegger, M.; Thalhammer, T.; Szekeres, T.; Jaeger, W. Metabolism of resveratrol in breast cancer cell lines: impact of sulfotransferase 1A1 expression on cell growth inhibition. *Cancer Lett.* **2008**, *261*, 172–182.

(25) van Ginkel, P. R.; Darjatmoko, S. R.; Sareen, D.; Subramanian, L.; Bhattacharya, S.; Lindstrom, M. J.; Albert, D. M.; Polans, A. S. Resveratrol inhibits uveal melanoma tumor growth via early mitochondrial dysfunction. *Invest. Ophthalmol. Vis. Sci.* **2008**, *49*, 1299–1306.

(26) Asensi, M.; Medina, I.; Ortega, A.; Carretero, J.; Bano, M. C.; Obrador, E.; Estrela, J. M. Inhibition of cancer growth by resveratrol is related to its low bioavailability. *Free Radical Biol. Med.* **2002**, *33*, 387–398.

(27) Soto, B. L.; Hank, J. A.; Van De Voort, T. J.; Subramanian, L.; Polans, A. S.; Rakhmilevich, A. L.; Yang, R. K.; Seo, S.; Kim, K.; Reisfeld, R. A.; Gillies, S. D.; Sondel, P. M. The anti-tumor effect of resveratrol alone or in combination with immunotherapy in a neuroblastoma model. *Cancer Immunol. Immunother.* **2011**, Feb 22 (Epub).